7174 *Inorg. Chem.* **2009**, *48*, 7174–7180
DOI: 10.1021/ic9003092

Inorganic Chemistry
Article

Two *EE*-Azido-Bridged Nickel(II) Layered Compounds: Vigorous Twisted Torsion Angle Ni−N_3−Ni Results in Ferromagnetic Behavior

Ru-Yin Li, Bing-Wu Wang,* Xin-Yi Wang, Xiu-Teng Wang, Zhe-Ming Wang, and Song Gao*

Beijing National Laboratory for Molecular Sciences, State Key Laboratory of Rare Earth Materials Chemistry and Applications, College of Chemistry and Molecular Engineering, Peking University, Beijing 100871, People's Republic of China

Received February 16, 2009

Two coordination polymers, Ni(endi)$(N_3)_2$ (endi = 1,2-bis(tetrazol-1-yl)ethane) (**1**) and Ni(4-acpy)$_2(N_3)_2$ (4-acpy = 4-acetylpyridine) (**2**), are obtained by employing a couple of cobalt complex as references. Both compounds have similar 2D (4,4) *EE* azide-nickel layer structures, but different interlayer separations. Their *EE* azide bridges are vigorously twisted, with the torsion angle τ value 88.3° and 107.6° for **1** and 89.2° for **2**. Different from most *EE* azide compounds, ferromagnetism is distinctly present, ordering below T_c = 25 K for **1** and T_c = 23 K for **2**. Fitting of magnetic susceptibility data using the spin Hamiltonian $H = -2J\sum S_1S_2$ gives the ferromagnetic intralayer coupling J = 14.70(6) cm^{-1} for **1** and 14.32(0) cm^{-1} for **2**, respectively. The magnetostructural correlations of **1** have been calculated using the density function theory based method. The computational results are consistent with the trend of the experimental data. One possible mechanism was proposed to explain the emergence of ferromagnetism based on the theoretical studies, and the ferromagnet construction approach was also proposed accordingly.

Introduction

Azide has been widely employed as short bridge to construct coordination complexes for its ability to transmit magnetic coupling. Some magnetostructural correlations have been summarized for different metal ions and bridging modes based on experimental and theoretical research. In most metal-azide coordination polymers, *EE* (End-to-End) azide generally transmits antiferromagnetic (AFM) coupling, but *EO* (End on) azide does not.[1,2] It was revealed by theoretical research that for the first-row ions the structural dependence of magnetic coupling is governed by the $d_{x^2-y^2}$ orbital energy gap, while d_{z^2} makes few or no contributions.[1] The overlap, orthogonality or mixed state of related orbitals, decides the nature of the magnetic superexchange interaction. The magnitude of superexchange is determined by several geometry parameters, such as the bond length, the bridging angle α (M−N−N), the torsion angle τ (M−*EE*-N_3−M) (Scheme 1), the dihedral angle δ for double bridges.[3−5] Either individual changes or their cooperated alteration would modify the intensity of the magnetic coupling. For *EE* azide, α and τ are important factors in determining the magnitude of the superexchange interaction. AFM (antiferromagnetic) coupling will be strongest when α is around 108° with a zero τ angle and becomes moderate upon an increase and decrease of α. However, the effect of α angle change is less dominant than τ. For their M−*EE*-N_3−M fragment, the value varies from 0° to 180° clockwise; the conformation gets twisted most with τ = 90° and is planar at τ = 0° (*cis*) or 180° (*trans*). The twist of the τ angle could induce a fast displacement of neighboring orbitals and invokes serious weakening of AFM coupling.

The electronic states of these compounds are also influenced by the change of geometry factors. Take a compound with *EE* azide bridge as an example; the filling of the d orbital of the metal ion brings more possible pathways to transmit a superexchange interaction. For d^6 and d^7 ions, the variation of the magnetic coupling was mainly influenced by the change of α and τ, especially τ. The anisotropy emerges by decreasing the coordination symmetry. For the d^9 system, the bond length and departure from the basal plane could be considered additionally.

In this work, we attempt to synthesize a series of *EE*-azido-bridged transition metal coordination polymers with analogous crystal structures and desired coordination environment, but different metal ions, to study the magnetostructural correlations in *EE*-azido-bridged transition metal complexes, especially the influence of the parameter τ on their magnetic properties.

*To whom correspondence should be addressed. Fax: (+86)10-62751708. E-mail: bwwang@pku.edu.cn (B.-W.W.), gaosong@pku.edu.cn (S.G.).

(1) Biani, F. F. d.; Ruiz, E.; Cano, J.; Novoa, J. J.; Alvarez, S. *Inorg. Chem.* **2000**, *39*, 3221.
(2) Ruiz, E.; Cano, J.; Alvarez, S.; Alemany, P. *J. Am. Chem. Soc.* **1998**, *120*, 11122.
(3) Escuer, A.; Vicente, R.; Ribas, J.; Fallah, M. S. E.; Solans, X.; Font-Bardla, M. *Inorg. Chem.* **1993**, *32*, 3727.
(4) Cortés, R.; Urtiaga, K.; Lezama, L.; Pizarro, J. L.; Goili, A.; Arriortua, M. I.; Rojo, T. *Inorg. Chem.* **1994**, *33*, 4009.
(5) Escuer, A.; Vicente, J. R.; Ribas, J.; Fallah, M. S. E.; Solam, X.; Font-Bardía, M. *Inorg. Chem.* **1994**, *33*, 1842.

 Published on Web 07/01/2009

Scheme 1. Definition of Torsion Angle (τ)

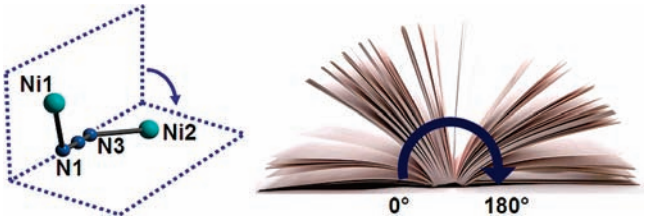

In the series of first-row transition metals, the Co(II) ion is very similar to the Ni(II) ion in radius and coordination behavior. They often form isomorphous compounds when the same ligands are employed[6−9] and are capable of synthesizing molecular alloys in different ratios.[10] Two Co compounds, Co(endi)$(N_3)_2$ (endi = 1,2-bis(tetrazol-1-yl)ethane) and Co(4-acpy)$_2(N_3)_2$ (4-acpy = 4-acetylpyridine), were obtained in previous work, both consisting of (4,4) layers of Co nodes linked by *EE* azido bridges. Their *EE* azido bridges are vigorously twisted, with the τ values of 107.97° and 75.19° for Co(endi)$(N_3)_2$ and 89.3° for Co(4-acpy)$_2(N_3)_2$, respectively.[11−13] In both compounds, AF couplings are transmitted through the *EE* azide, and weak ferromagnetic and AF ordering are reached under the critical temperatures 9 and 11 K, respectively. Similar structures have been observed in Mn compounds too.[14,15] In this work, the Ni(II) ion instead of Co(II) and endi and 4-acpy as the co-ligands are used to obtain isomorphous compounds with twisted torsion angles. Two azido-bridged Ni(II) compounds, Ni(endi)$(N_3)_2$- (**1**) and Ni(4-acpy)$_2(N_3)_2$ (**2**), are indeed isomorphous with their Co(II) analogues, as expected. Distinct magnetic properties are exhibited with the critical temperatures of 25 K for **1** and 23 K for **2**, respectively. Theoretic calculations have been performed on model structure **1** and revealed the magnetostructural correlations in this kind of 2D *EE*-azido-bridged Ni(II) layered compounds, providing us a useful strategy to design more new magnetic coordination complexes that can fulfill the requirements for both structure and magnetism.

Experimental Section

Synthesis. All starting materials were commercially available at analytical grade and used without further purification.

CAUTION! *Although not encountered in our experiment, azido salts and complexes of metal ions are potentially explosive. Only a small amount of materials should be prepared, and handled with care.*

Preparation of Ni(endi)$(N_3)_2$, 1. Single crystals were obtained by diffusion. A DMF solution (5 mL) of NaN_3 (1.0 mmol) and endi (0.5 mmol) was put into a clean test tube. Then an aqueous solution (5 mL) of Ni$(ClO_4)_2$ (0.5 mmol) was carefully laid on top. The test tube was allowed to stand undisturbed at room temperature in the dark for three months. Bottle-green prism crystals were obtained (yield: 30%). IR (cm^{-1}): $\nu_{as}(N_3)$, 2070 (vs), ν(C−H), 3100 (ms), $\nu_s(N_3)$, 1370 (ms), and 1320 (m). Anal. Calcd for $NiN_{14}C_4H_6$ (%): C, 15.45; N, 63.07; H, 2.59. Found: C, 15.52; N, 63.94; H, 2.11.

Table 1. Crystallographic Data and Structure Refinement for **1**·Ni and **2**·Ni

	1·Ni	**2**·Ni
formula	$C_4H_6NiN_{14}$	$C_{28}H_{28}Ni_2N_{16}O_4$
fw	308.94	770.01
cryst syst	triclinic	monoclinic
space group, Z	$P\bar{1}$, 2	$P2_1/c$, 1
a [Å]	6.5631(2)	11.8326(4)
b [Å]	9.0899(3)	8.2663(3)
c [Å]	9.4638(3)	8.0851(7)
α [deg]	74.7030(11)	
β [deg]	87.8600(11)	91.930(2)
γ [deg]	70.229(2)	
V [Å^3]	511.65(3)	790.37(8)
r_{calcd} [g cm^{-3}]	2.005	1.618
μ [mm^{-1}]	1.913	1.255
$R_1{}^a$ [$I > 2\sigma(I)$]	0.0313	0.0355
$wR_2{}^b$ (all data)	0.0699	0.0729
GOF	0.942	0.917

$^aR_1 = \sum||F_o| - |F_c||/\sum|F_o|$. $^bwR_2 = \{\sum[w(F_o^2 - F_c^2)^2]/\sum[w(F_o^2)^2]\}^{1/2}$.

Preparation of Ni(4-acpy)$_2(N_3)_2$, 2. An aqueous solution (10 mL) of Ni$(CH_3COO)_2$ (0.5 m mol) was added in the DMF solution (5 mL) of 4-acpy (1.0 mmol). After 4 h stirring, NaN_3 (1.0 mmol) was added in. The resulting clear solution was left to stand at room temperature. Green, thin plate crystals were harvested the next day in a yield of 50%. IR (cm^{-1}): $\nu_{as}(N_3)$, 2070 (vs), ν_{as}(C═O), 1700 (ms), $\nu_{as}(N_3)$, 1370 (ms), and 1320 (m). Anal. Calcd for $C_{14}H_{14}N_8O_2Ni$ (%): C, 43.67; N, 29.10; H, 3.66. Found: C, 43.45; N, 29.26; H, 3.61.

X-ray Crystallography and Physical Measurements. Crystallographic data of **1** and **2** were collected at 293 K on a Nonius KappaCCD diffractometer with graphite-monochromated Mo Kα radiation (λ = 0.71073 Å).[16,17] Empirical absorption corrections were applied using the Sortav program.[18,19] The structures were solved by the direct method and refined by full-matrix least-squares method on F^2 with anisotropic thermal parameters for all non-hydrogen atoms using the SHELX-97 program.[20,21] Hydrogen atoms were added geometrically and refined using the riding model. Crystallography data and refinement results are listed in Table 1, and selected bond lengths and angles in Table 2.

CCDC-714905 (**1**) and CCDC-714904 (**2**) contain the supplementary crystallographic data for this paper. These data can be obtained free of charge from the Cambridge Crystallographic Data Centre via www.ccdc.cam.ac.uk/data_request/cif. A CIF file of **1** and **2** can also be found in the Supporting Information.

Elemental analyses were carried out on an Elementary Vario EL analyzer. IR spectra were recorded on a Nicolet Magna-IR 750 spectrometer equipped with a Nic-Plan microscope against pure samples.

(6) Wang, Z. M.; Zhang, B.; Inoue, K.; Fujiwara, H.; Otsuka, T.; Kobayashi, H.; Kurmoo, M. *Inorg. Chem.* **2007**, *46*(2), 437.
(7) Toma, L. M.; Toma, L. D.; Delgado, F. S.; Ruiz-Pérez, C.; Sletten, J.; Cano, J.; Clemente-Juan, J. M.; Lloret, F.; Julve, M. *Coord. Chem. Rev.* **2006**, *250*, 2176.
(8) Hearns, N. G. R.; Hesp, K. D.; Jennings, M.; Korčk, J. L.; Preuss, K. E.; Smithson, C. S. *Polyhedron* **2007**, *26*, 2047.
(9) Murugavel, R.; Krishnamurthy, D.; Sathiyendiran, M. *J. Chem. Soc., Dalton Trans.* **2002**, *34*.
(10) Zeng, M. H.; Wang, B.; Wang, X. Y.; Zhang, W. X.; Chen, X. M.; Gao, S. *Inorg. Chem.* **2006**, *45*, 7069.
(11) Wang, X. Y.; Wang, Z. M.; Gao, S. *Inorg. Chem.* **2008**, *47*, 5720.
(12) Abu-Youssef, M. A. M.; Mautner, F. A.; Vicente, R. *Inorg. Chem.* **2007**, *46*, 4654.
(13) Li, R. Y.; Wang, X. Y.; Liu, T.; Xu, H. B.; Zhao, F.; Wang, Z. M.; Gao, S. *Inorg. Chem.* **2008**, *47*, 8134.
(14) Escuer, A.; Vicente, R.; Goher, M. A. S.; Mautnero, F. A. *Inorg. Chem.* **1995**, *34*, 5707.
(15) Escuer, A.; Vicente, R.; Goher, M. A. S.; Mautner, F. A. *Inorg. Chem.* **1996**, *35*, 6386.
(16) *Collect* data collection software; Nonius B.V.: Delft, The Netherlands, **1998**.
(17) *HKL2000* and *maXus* software; University of Glasgow, Scotland, UK, Nonius BV, Delft, The Netherlands, and MacScience Co. Ltd., Yokohama, Japan, **2000**.
(18) Blessing, R. H. *Acta Crystallogr.* **1995**, *A51*, 33.
(19) Blessing, R. H. *J. Appl. Crystallogr.* **1997**, *30*, 421.
(20) Sheldrick, G. M. *SHELXTL Version 5.1.*; Bruker Analytical X-ray Instruments Inc.: Madison, WI, **1998**.
(21) Sheldrick, G. M. *SHELX-97, PC Version*; University of Göttingen: Germany, **1997**.

Table 2. Selected Bond Lengths (Å) and Bond Angles (deg) for **1** and **2**[a]

1

Ni(1)−N(6)a	2.075(2)	Ni(1)−N(1)a	2.115(2)	Ni(1)−N(11)a	2.0861(19)
Ni(1)−N(11)	2.0860(19)	Ni(2)−N(7)b	2.0713(19)	Ni(2)−N(3)b	2.104(2)
N(7)−Ni(2)−N(7)b	180	N(3)b-Ni(2)−N(4)b	91.46(8)	N(9)−N(8)−N(7)	109.83(19)
N(3)b−Ni(2)−N(3)	180	N(7)b−Ni(2)−N(3)b	91.59(8)	N(13)−N(12)−N(11)	110.14(17)
N(11)a−Ni(1)−N(1)	86.06(8)	N(11)−Ni(1)−N(1)	93.94(8)	N(9)−N(10)−C(2)	120.61(19)
N(7)−Ni(2)−N(3)b	88.41(8)	C(1)−N(7)−N(8)	105.98(19)	N(13)−N(14)−C(3)	120.94(18)
N(3)−Ni(2)−N(4)b	88.54(8)	C(4)−N(11)−N(12)	106.00(17)	N(12)−N(11)−Ni(1)	122.45(13)
N(7)b−Ni(2)−N(4)b	88.59(8)	N(12)−N(13)−N(14)	106.66(17)	N(5)−N(4)−Ni(2)	122.62(16)
N(6)a−Ni(1)−N(1)a	88.86(8)	N(8)−N(9)−N(10)	107.03(18)	N(8)−N(7)−Ni(2)	126.47(15)
N(6)−Ni(1)−N(11)a	89.80(8)	C(1)−N(10)−N(9)	107.9(2)	C(1)−N(7)−Ni(2)	127.43(16)
N(6)a−Ni(1)−N(11)a	90.20(8)	C(4)−N(14)−N(13)	108.29(17)	C(4)−N(14)−C(3)	130.8(2)
N(6)a-Ni(1)−N(1)	91.14(8)	N(11)−C(4)−N(14)	108.9(2)	C(4)−N(11)−Ni(1)	131.49(16)
N(6)a-Ni(1)−N(6)	180.00(17)	N(1)c−N(2)−N(3)	175.7(2)	C(1)−N(10)−C(2)	131.5(2)
N(1)−Ni(1)−N(1)a	180.00(7)	N(4)−N(5)−N(6)	176.8(2)	N(2)−N(3)−Ni(2)	132.58(17)
N(2)e−N(1)−Ni(1)	143.32(16)	N(11)−Ni(1)−N(11)a	180.00(14)	N(5)−N(6)−Ni(1)	135.99(17)

2

Ni(1)−N(1)f	2.090(2)	Ni(1)−N(3)g	2.113(2)	Ni(1)−N(4)f	2.116(2)
N(1)f−Ni(1)−N(3)g	90.08(10)	N(1)f−Ni(1)−N(4)f	91.67(9)	N(3)g−Ni(1)−N(4)	90.88(8)
N(1)f−Ni(1)−N(3)h	89.92(10)	N(1)−Ni(1)−N(4)f	88.33(9)	N(3)h−Ni(1)−N(4)	89.12(8)
N(3)g−Ni(1)−N(3)h	180.00(12)	N(3)g−Ni(1)−N(4)f	89.12(8)	N(4)f−Ni(1)−N(4)	180
N(1)−Ni(1)−N(4)	91.67(9)	N(3)h−Ni(1)−N(4)f	90.88(8)	N(2)−N(3)−Ni(1)i	127.5(2)

[a]Symmetry transformations used to generate equivalent atoms: a $-x,-y,-z$; b $-x+1,-y,-z-1$; c $x,y,z-1$; d $-x+1,-y-1,-z$; e $x,y,z+1$; f $-x,-y+1,-z$; g $x,-y+3/2,z-1/2$; h $-x,y-1/2,-z+1/2$; i $-x,y+1/2,-z+1/2$.

Table 3. Summary of Structure Parameters and Magnetic Properties of **1**, **2**, and Their Corresponding Co(II) Compounds

	cryst syst	$M-N_{azide}$	intralayer M−M (Å)	interlayer M−M (Å)	α (deg)	τ (deg)	J (cm^{-1})	T_c (K)	ref
$Co(endi)(N_3)_2$	triclinic	2.09, 2.11, 2.13, 2.14, 2.07, 2.10	5.74	8.68	123.6, 136.7 140.1, 145.1	107.9, 75.2	−3.5	7.8	13
1 $Ni(endi)(N_3)_2$	triclinic	2.11, 2.11	5.85, 5.65	8.60	122.6, 132.6 136.0, 143.4	88.3, 107.6	14.70(6)	25	this work
$Co(4\text{-acpy})_2(N_3)_2$	monoclinic	2.12, 2.13	5.84	11.73	128.2, 149.1	84.9	−2.64	11.2	11
2 $Ni(4\text{-acpy})_2(N_3)_2$	monoclinic	2.11, 2.09	5.78	11.83	127.5, 146.4	89.2	14.32(0)	23	this work

Magnetic data of compounds were measured on a Quantum Design MPMS-XL5 SQUID system. The experimental susceptibility data were corrected for diamagnetism (Pascal's parameters) and background by experimental measurement on the sample holder.[22] Heat capacity measurements were carried out on a Quantum Design PPMS system. To verify the absolute heat capacity values, adiabatic calorimetry measurements were done using a laboratory-made apparatus.[23]

Theoretical Calculations. Density functional theory based calculations combined with the broken symmetry method[24] were performed on **1** using ADF program package version 2007.1 with a dimer fragment model,[25,26] as shown in the Figure S1. General gradient approximation (PBE exchange−correlation functional[27]) was used beyond the local density approximation (VWN exchange−correlation functional) in all the calculations.[28] The spin Hamiltonian $H = -2JS_1S_2$ described above was employed, and the magnetic coupling constant J value was deduced with the calculated energy difference $E_{HS} - E_{BS}$.

$$S_{max}{}^2 J_{12} = E_{BS} - E_{HS}$$

where S_{max} is the maximal spin multiplet of the system studied; E_{BS} and E_{HS} are the expected energy value of the broken symmetry state (BS) and the energy eigenvalue of the highest spin state (HS), respectively.

Results and Discussion

Crystal Structures. Crystals of **1** and **2** were obtained by the reaction of Ni(II) salts, NaN_3, and co-ligands. Their synthesis methods refer to the corresponding Co compounds (see Experimental Section).[11,13] Both structures possess the (4,4) layers of Ni nodes bridged by *EE* azido bridges. This kind of azido-Ni layered structure is rare; only one similar compound has been synthesized by Maier et al.[29] Crystallographic data are summarized in Table 1, and selected bond distances and angles are listed in Table 2. In general, Ni(II) is slightly smaller than Co(II), so the lattice constants of axes and volume and the related interatomic distances of the

(22) Boudreaux, E. A., Mulay, J. N., Eds. *Theory and Application of Molecular Diamagnetism*; J. Wiley and Sons: New York, 1976.
(23) Kume, Y.; Miyazaki, Y.; Matsuo, T.; Suga, H. *J. Phys. Chem. Solids* **1992**, *53*, 1297.
(24) Noodleman, L.; A.Case, D.; Aizman, A. J. *J. Am. Chem. Soc.* **1988**, *110*, 1001.
(25) Amsterdam Density Functional (ADF), version 2005.01.
(26) *ADF, Scientific Computing and Modeling*, Theoretical Chemistry, Vrije Universiteit: Amsterdam, **2005**.
(27) Perdew, J. P.; Burke, K.; Ernzerhof, M. *Phys. Rev. Lett.* **1996**, *77*, 3685.
(28) Vosko, S. H.; Wilk, L.; Nusair, M. *Can. J. Phys.* **1980**, *58*, 1200.
(29) Maier, H. E.; Krischner, H.; Paulus, H. *Z. Kristallogr.* **1981**, *157*, 277.

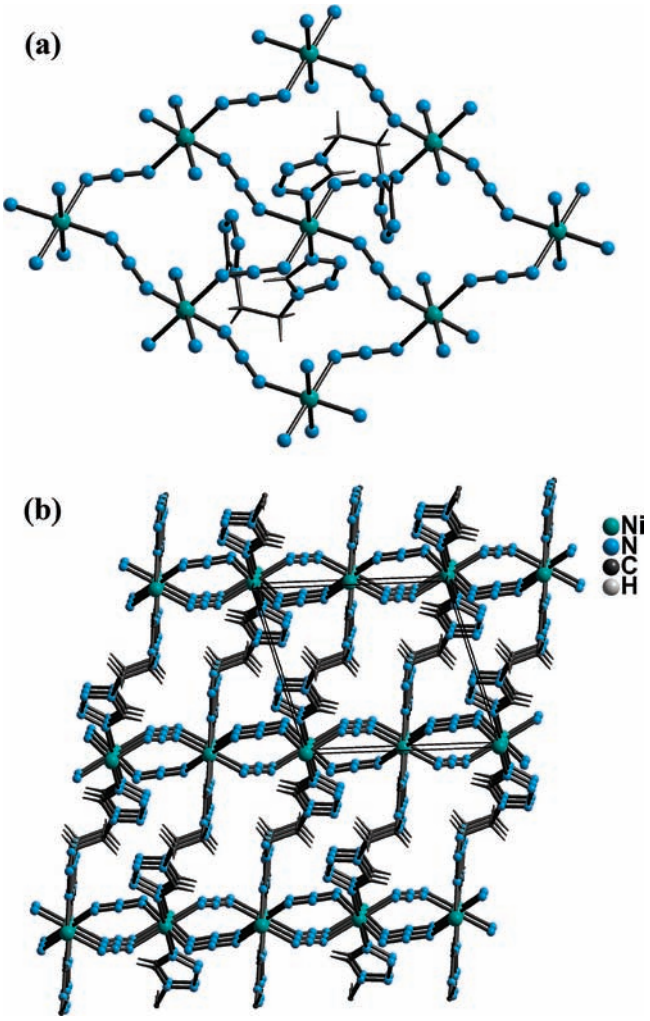

Figure 1. (a) Perspective view of 2D azido-bridged Ni(II) layers of **1**. (b) Perspective view of 3D network of compound **1**.

Ni compounds are all slightly smaller than those of the Co compounds (Table 3).[11,13]

Ni(endi)$(N_3)_2$ (1). 1 crystallized in the triclinic space group $P\bar{1}$. It is a 3D coordination network consisting of Ni-*EE*-azido (4,4) sheets that are connected by bridge ligands endi (Figure 1), like its Co analogue.[13] There are two crystallographically independent Ni(II) ions located at the inversion centers, one at (0, 0, 0) (Ni1) and the other at (0.5, 0, −0.5) (Ni2). Both possess octahedral coordination symmetry (Figure S1 in the Supporting Information), with four equatorial *EE* azido ions and two axial endi ligands. The $Ni1N_6$ octahedron is elongated along one of the $N1_{azide}-Ni1-N1_{azide}$ direction (Figure S1 in the Supporting Information), with the two long Ni−N distances of 2.115 Å and the short ones of 2.075 to 2.086 Å. The *cis* N−Ni1−N angle of $Ni1N_6$ varies from 86.06° to 93.94°, and all *trans* N−Ni−N angles are 180.00° (Table 2). The coordination geometry around Ni2 is a compressed octahedron along the $N3_{endi}-Ni2-N3A_{endi}$ direction, with the two short Ni−N distances of 2.071 Å and the four long ones of 2.104 Å. The *cis* N−Ni2−N angles are 88.41−91.46°, and all *trans* N−Ni2−N

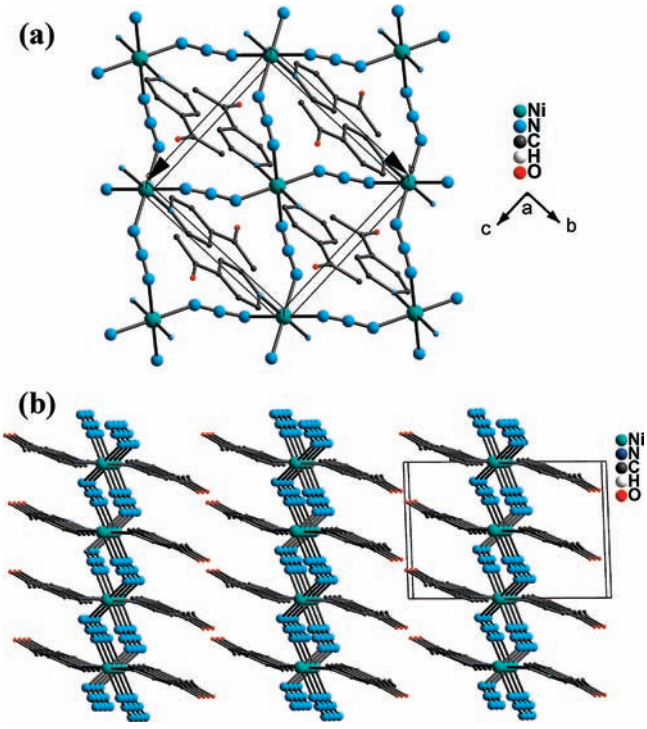

Figure 2. (a) Perspective view of 2D azido-bridged Ni(II) layers of **2**. (b) Perspective view of 3D network of compound **2**.

angles are 180.00°. The Ni−N distances are in the range of the reported Ni-azide compounds.[3,30−33]

The two unique *EE* azide ions are nearly linear, with N−N−N angles of 175.70° and 176.80°, respectively. The bridging angles, α, formed by Ni(II) and the azide ions are in the range 132.58° to 143.32°, and the two τ angles are 88.31° and 107.58°, respectively. Through the *EE* azido ligands, the neighboring Ni nodes are connected into a 2D (4,4) sheet along the *ac* plane (Figure 1a). This kind of sheet has been observed in many metal-azide compounds[11−15,34−37] but only one example for Ni(II), as mentioned above.[29] The two unique intralayer Ni···Ni distances spanned by *EE*-azido ions are 5.657 and 5.858 Å, respectively. The bridge ligands endi adopt a *gauche* conformation with N−C−C−N torsion angles of 61.11°, linking the neighboring Ni-*EE*-azido (4,4) sheets along the *b* direction into the 3D framework of NaCl type (Figure 1b). The shortest interlayer Ni···Ni distance is 8.606 Å.

Ni(4-acpy)$_2$$(N_3)_2$ (2). 2 belongs to the monoclinic space group $P2_1/c$ (Table 1). It consists of 2D (4,4) Ni-*EE*-azido sheets that are very similar to **1** (Figure 2, S2 in the Supporting Information). There is only one crystallographically unique Ni(II) ion at the inversion center

(30) McLachlan, G. A.; Fallon, G. D.; Martin, R. L.; Moubaraki, B.; Murray, K. S.; Spiccia, L. *Inorg. Chem.* **1994**, *33*, 4663.
(31) Monfort, M.; Resino, I.; Ribas, J.; Solans, X.; Font-Bardia, M.; Stoeckli-Evans, H. *New J. Chem.* **2002**, *26*, 1601.
(32) Monfort, M.; Ribas, J.; Solans, X.; Font-Bardía, M. *Inorg. Chem.* **1996**, *35*, 7633.
(33) Vicente, R.; Escuer, A.; Ribas, J.; Fallah, M. S. E.; Solans, X.; Font-Bardía, M. *Inorg. Chem.* **1995**, *34*, 1278.
(34) Goher, M. A. S.; Abu-Youssef, M. A. M.; Mautner, F. A.; Vicente, R.; Escuer, A. *Eur. J. Inorg. Chem.* **2000**, 1819.
(35) Doi, Y.; Ishida, T.; Nogami, T. *Bull. Chem. Soc. Jpn.* **2002**, *75*, 2445.
(36) Ma, B. Q.; Sun, H. L.; Gao, S.; Su, G. *Chem. Mater.* **2001**, *13*, 1946.
(37) Escuer, A.; Vicente, R.; Goher, M. A. S.; Mautner, F. A. *J. Chem. Soc., Dalton Trans.* **1997**, 4431.

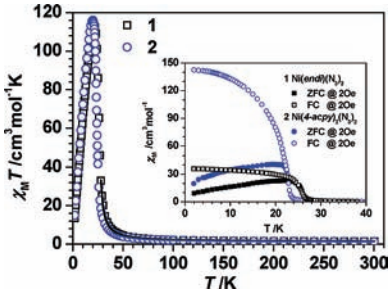

Figure 3. Plots of $\chi_M T$ vs T for **1** and **2** under an applied field of 1 kOe. Inset: FC and ZFC magnetization versus T plots at 2 Oe of **1** and **2**.

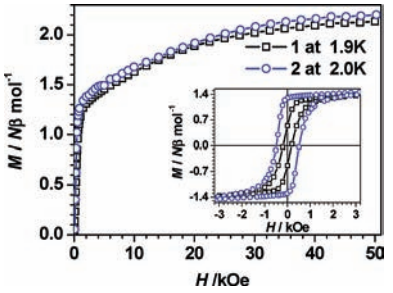

Figure 4. Plots of M vs H for **1** and **2**. Inset: the hysteresis loop of **1** and **2**.

(0, 0.5, 0). The Ni(II) ion, which is coordinated by four nitrogen atoms from azido ligands and two nitrogen atoms of the co-ligand 4-acpy, adopts a compressed octahedral geometry along the $N1_{azide}$−Ni−$N1A_{azide}$ direction (Figure S2 in the Supporting Information). The molecular geometry parameters around Ni(II) are Ni−N_{azide} = 2.090−2.113 Å, Ni−N_{acpy}= 2.116 Å, *cis* N−Ni−N angles = 88.33−91.67°, and *trans* N−Ni−N angles = 180.00° (Table 2). All of Ni(II) ions are connected by *EE* azido ions into a neutral 2D layer with (4,4) topology along the *bc* plane, with a unique interlayer distance Ni···Ni = 5.781 Å. The grids on this layer are almost perfect squares. The bridging angles are 127.55° and 146.43°, and the τ is 89.16°, similar to that found in compound **1**. The coordinated 4-acpy acts as a terminal ligand and sticks out of the layer. The neighboring layers are stacked along the *a* axis, and no H-bonds were observed between the layers. The nearest interlayer Ni···Ni distance is 11.833 Å.

Magnetic Properties. As discussed above, both compounds consist of (4,4) Ni-*EE*-azido layers well separated by the interlayer co-ligands. They could be considered as a 2D magnetic system although **1** is actually a structural 3D framework. As the two materials have similarity in their 2D layer structures and in details in their structural parameters, especially similar bridging angles (α) and twisted torsion angles (τ), similar magnetic behaviors would be expected.

The thermal variations of the magnetic susceptibility per Ni for **1** and **2** were measured from 2 to 300 K under 1 kOe magnetic field (Figure 3). The room-temperature values of $\chi_M T$ for **1** and **2** are 1.37 and 1.36 cm^3 mol^{-1} K, respectively; both are appreciably higher than that expected for spin-only Ni(II) ions. Upon cooling, both $\chi_M T$ values exhibited a slow increase in the lower temperature region, then rose up rapidly and reached a maximum of ca. 120 cm^3 mol^{-1} K at 19 K for **1** and 21 K for **2**, respectively. After that, the curves decreased upon further cooling because of magnetic saturation effects. The high-temperature magnetic data obeyed the Curie−Weiss law ($\chi_M = C/(T-\theta)$, Figure S3 in the Supporting Information), with C = 1.17(3) cm^3 mol^{-1} K and θ = 45.81(7) K for **1**, and C = 1.16(3) cm^3 mol^{-1} K and θ = 42.93(7) K for **2**, respectively. The positive values of θ indicated FO couplings between Ni(II) ions. On the basis of the (4,4) layer structures of Ni-azide in **1** and **2**, Lines's model[38] for a square lattice of Ni(II) was used to fit the high-temperature susceptibility data (30 to 300 K for **1** and 40 to 300 K for **2**), as eq 1.

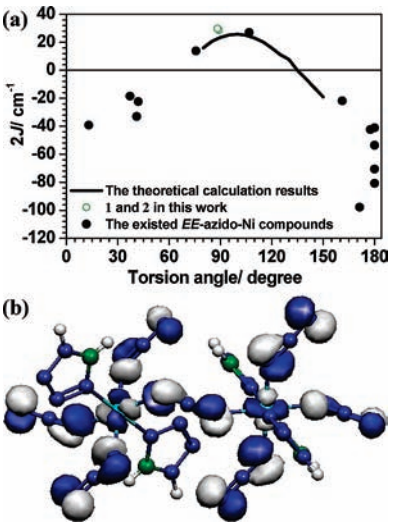

Figure 5. (a) Diagram of magnetic coupling for a (N5)Ni−N_3−Ni(N5) system of **1** as a function of the variation of the torsion angle. The dots represent the experimental data. (b) Perspective of the selected MOs showing the main σ (180°) and π (90°) superexchange pathway.

$$\chi_M = \frac{Ng^2\beta^2}{J}\left(3x + \sum_{n=1}^{6}\frac{C_n}{x^{n-1}}\right)^{-1} \quad (1)$$

The interlayer interaction was estimated by the mean-field model, as shown in eq 2.

$$\chi_M' = \frac{\chi_M}{1 - \frac{2zJ'\chi_M}{N\beta^2 g^2}} \quad (2)$$

with $x = k_B T/JS(S+1)$, C1 = 4.0, C2 = 1.834, C3 = 0.445, C4 = 0.224, C5 = 0.132, C6 = 0.019, together with the consideration of the interlayer interaction (zJ') using the mean-field approximation. The best fits produced g = 2.18 and J = 14.70(6) cm^{-1} for **1** and g = 2.12 and J = 14.32(0) cm^{-1} for **2**, zJ' = 1.37(2) cm^{-1} for **1** and 1.68(3) cm^{-1} for **2**, and the reliability factors $R = 3.5 \times 10^{-4}$ (**1**) and 6.8×10^{-6} (**2**) (R defined as $\sum_i[(\chi_M T)_{obs} - (\chi_M T)_{calc}]^2/\sum_i[(\chi_M T)_{obs}]^2$)). These results revealed the FO magnetism within the materials.

The two materials were further characterized in the low-temperature region by different measurements, including zero-field-cooled magnetization (ZFCM) and field-cooled magnetization (FCM) in a low field of 2 Oe (Figure 3, inset), isothermal magnetization (Figure 4), a preliminary specific

(38) Lines, M. E. *J. Phys. Chem. Solids* **1970**, *31*, 101.

Table 4. Summary of Structure Parameters and Magnetic Properties of *EE*-Azide-Bridged Ni(II) Compounds

	α (deg)	τ (deg)	*g*	*J* (cm^{-1})	T_c (K)	ref
catena-(μ-N_3)[Ni(1,4,8,11-tetraazacyclotetradecane)](ClO_4)·H_2O	140.7(3), 128.2(3)	13.1	2.22	−39.2		3
[Ni_2(trenpy)$_2$(μ-N_3)]($C1O_4$)$_3$	131.6(5)	0 (180)	2.24	−53.6		30
trans-[Ni(N-Pren)$_2$($\mu_{1,3}$-N_3)]$_n$(ClO_4)$_n$	136.4(3), 149.8(3)	161.2	2.27	−21.8		31
trans-[Ni(N,N′-Pren)$_2$($\mu_{1,3}$-N_3)]$_n$(PF_6)$_n$	136.5, 145.4	177.6	2.34	−42.3		31
[Ni(1,3-diamino-2,2-dimethylpropane)$_2$(μ-N_3)]$_n$(PF_6)$_n$	136.5	0 (180)	2.29	−41.1		32
[Ni(1,3-diaminopropane)$_2$(μ-N_3)]$_n$(PF_6)$_n$	126.1	0 (180)	2.36	−70.6		32
[{Ni(Me_2[14]-1,3-dieneN$_4$)(μ-N_3)}$_n$](ClO_4)$_n$	115.67(1), 116.8(2)	171.3	2.29	−97.8		33
[Ni(bipy)$_2$(N_3)](ClO_4)	120.1(6) to 126.6(6)	46.1 and 41.1	2.15	−33.0		4
[Ni(bipy)$_2$(N_3)](PF_6)	120.6(6) to 127.4(6)	45.1 and 42.0	2.15	−22.4		4
trans-[Ni(333-tet)(μ-N_3)$_n$](ClO_4)$_n$	123.6(2), 142.4(3)	0 (180)	2.40	−80.7		5
cis-[Ni(333-tet)(μ-N_3)](PF_6)$_n$	151.8(1),151.3(1)	37.2	2.29	−18.5		5
[Ni_2(L1)(N_3)(H_2O)][CF_3SO_3]$_3$·4H_2O	165.8			11.82		39
[Ni_2(L1)(N_3)][ClO_4]$_3$·MeCN·2H_2O				7.72		39
[{Ni(5-methylpyrazole)$_4$(N_3)}$_n$](ClO_4)$_n$·nH_2O	128.4, 146.1	75.7	2.21	6.91		40, 41
[Ni(μ-N_3)$_2$(N,N-Et_2-N′-Me-en)]$_n$	137.0, 144.3	110.4			16	42
[Ni(L)(N_3)$_2$]$_n$	124.5	106.8		13.5	5	43
1	122.6 to 143.4	88.3, 107.6	2.18	14.70	25	this work
2	127.5, 146.4	89.2	2.12	14.32	23	this work

heat capacity measurement under zero field (Figure S4 in the Supporting Information), and ac susceptibility (Figure S5 in the Supporting Information). The ZFCM/FCM data clearly defined the occurrence of long-range ordering (LRO) by the bifurcation and the sharp increase of FCM plots below 26 K for **1** and 23.4 K for **2**, and the negative peak of the derivative d(FCM)/dT is 25.9 K (**1**) and 22.9 K (**2**). The isothermal magnetization at ca. 2 K increased quickly to 1.4 Nβ at 2 kOe and gradually saturated to slightly above 2 Nβ, as expected for a $S = 1$ spin system. Hysteresis loops were observed for the two compounds, with a coercivity of 200 Oe for **1** and 500 Oe for **2**, respectively. These dc measurements confirmed the FO LRO of the two materials. The preliminary specific heat (C_P) data also confirmed the LRO of FO by the cusps appearing around 25 K for **1** and 23 K for **2**, which correspond with the peak value of d(FCM)/dT. Finally, the temperature dependence of ac susceptibilities of **1** and **2** under a zero applied dc field revealed response peaks around T_C in both in-phase χ_M' and out-of-phase χ_M'', and they were all frequency-independent, indicating the occurrence of LRO. It is noted that below the T_C, new peaks emerged around 10 K in the ac response for all measurement frequencies and display weak frequency dependency. These relaxation behaviors could be attributed to the domain wall movement within the two ferromagnets. Therefore, all results revealed the occurrence of FO LRO for these two Ni-*EE*-azide compounds.

Many compounds of *EE*-azido-bridged Mn(II) and Co(II) with (4,4) topology have been synthesized and characterized,[11−15,29,34−37] which all possess AF coupling through the *EE* azide. However, different properties, i.e., FO, are observed in the Ni compounds **1** and **2**. Table 3 summarizes the structural and magnetic parameters of **1** and **2** and their Co(II) analogues as references.[11−13] In comparison to the Co compounds, the Ni compounds have very similar structures, but different magnetic coupling (FO vs AF), higher critical temperature, higher magnetization, higher remanence, and larger coercivity.

Magnetostructural Correlations. *EE* azide ions transmit AF coupling in almost all reported *EE*-azido-bridged polymers; only five exceptions exist, in which ferromagnetic coupling interactions are transmitted. Two dinuclear nickel cryptates, [Ni_2(L_1)(N_3)(H_2O)][CF_3SO_3]$_3$·2H_2O·EtOH, in which the *EE* azido bridges transmit FO coupling were reported by Vicente.[39] By modulation of the cryptate, the azide bridges possess almost linear comformations with large α angles of around 165°, which is expected to be the critical value in the formation of orthogonality with zero torsion angle τ. A 1D azido-Ni chain, [{Ni(5-methylpyrazole)$_4$(N_3)}$_n$](ClO_4)$_n$·nH_2O, with *EE* azide bridges was reported that transmits FO coupling.[40,41] The chains have ordinary α values but a vigorously twisted τ angle (Ni−*EE*-N_3−Ni) of 75.7° and show an unusual "ferromagnetic spin canting" state. Monfort reported a ferromagnetic layered compound, [Ni(μ-N_3)$_2$(N,N-Et_2-N′-Me-en)]$_n$; the τ angle of its *EE* azide is 110.44°.[42] Chaudhuri obtained a ferromagnetic 1D chain, [Ni(L)(N_3)$_2$]$_n$, with a Schiff base. The τ angle is 106.8°.[43]

From the Ni(II) compounds mentioned above, it can be concluded that both linear *EE* azide with zero τ angle and the vigorously twisted *EE* azide could intensely weaken the AFM coupling, induce an incidental orthogonality of the $d_{x^2-y^2}$ orbital of metal ions,[3−5,14,39] and transmit FO coupling. The ferromagnetic properties of **1** and **2** could be attributed to this mechanism. Former theoretical calculations mainly focus on the magnetostructural correlations of AFM couplings transmitted by the *EE* azide, but the effect of incidental orthogonality of the *EE* azide that transmits ferromagnetic coupling has not been studied. So, we carried out density functional theory based calculations on a dimer fragment model of **1** to investigate the origin of ferromagnetic coupling from a theoretical viewpoint.

In this study, the values of J are calculated as a function of structural parameter τ. Hampered by the steric hindrance of the co-ligand in **1**, the calculations are carried out in a limited structural region. This provides a rough magnetostructural correlation of (4,4) *EE* azide-nickel layers. The resultant data of our calculations are plotted in Figure 5a and Figure 5b. Fixing the bridging angle, the increasing torsion angle induces

(39) Escuer, A.; Harding, C. J.; Dussart, Y.; Nelson, J.; McKee, V.; Vicente, R. *J. Chem. Soc., Dalton Trans.* **1999**, 223.
(40) Hong, C. S.; Do, Y. *Angew. Chem., Int. Ed.* **1999**, *38*, 193.
(41) Hong, C. S.; Koo, J. e.; Son, S. K.; Lee, Y. S.; Kim, Y. S.; Do, Y. *Chem.—Eur. J.* **2001**, *7*, 4243.
(42) Monfort, M.; Resino, I.; Ribas, J.; Stoeckli-Evans, H. *Angew. Chem., Int. Ed.* **2000**, *39*, 191.
(43) Mukherjee, P. S.; Dalai, S.; Zangrando, E.; Lloret, F.; Nirmalendu; Chaudhuri, R. *Chem. Commun.* **2001**, 1444.

a fast variation of the J curve. The J value stays positive, rapidly increases from 80°, and reaches a maximum at 100°, which was supposed to be 90° in the past.[42] Then it decreases gradually along with the increase of τ. The positive magnetic coupling constant gradually decays and became 0 cm^{-1} at 135°. The character of the magnetic coupling changes from FO to AF. A further decrease of J lasts upon a continuous increase of torsion angle between 135° and 150°, and the AF coupling gradually dominates the interactions. Although incomplete, the plot of J versus torsion angle is supposed to be symmetrical around the maximum. So, we can deduce that ferromagnetic coupling induced by incidental orthogonality would emerge when azide ions possess vigorously twisted conformations. Table 4 summarizes the reported *EE*-azido-bridged Ni(II) compounds, including which exhibit ferromagnetic couplings. Their experimental data are added in the J curve. Some *trans EE* azide bridges with $\tau = 180°$ conformations are considered as 0°.[5,30,32] It can be easily figured out that the trend of experimental data is consistent with the calculation results. The experimental maximum value deduced from it should be close to the calculated one also. **1** and **2** have the largest J value among them.

Conclusion

Taking the corresponding Co compounds as references, two isomorphous Ni azide compounds are synthesized. The vigorously twisted *EE* azide ions induce an incidental orthogonality between neighboring $d_{x^2-y^2}$ orbitals. Ferromagnetic coupling was transmitted by the *EE* azide, with the LRO under 25 and 23 K. Theoretical calculations have been carried out and shed light on the magnetostructural correlations of the *EE* azide. It is revealed that the τ angle is the key geometric factor to influence the character and magnitude of superexchange interactions. The change of τ could induce both FO and AF couplings between d^8 ions. AF coupling exists when the torsion angle is close to the planar conformation 0° or 180° and is easily weakened along the twist of the torsion angle toward 90°. Further twist of the τ angle results in FO coupling, which reaches a maximum at 100°. The theoretical calculation results are consistent with the trend of the experimental data. This magnetostructural correlation may help to construct more ferromagnetic Ni compounds easily by rational design.

Acknowledgment. This work was supported by the NSFC (20821091, 20503001) and the National Basic Research Program of China (Grant 2006CB601102, 2009CB929403).

Supporting Information Available: This material is available free of charge via the Internet at http://pubs.acs.org.